Electrochemical degradation of waters containing O-Toluidine on PbO$_2$ and BDD anodes

Emna Hmani, Sourour Chaabane Elaoud*, Youssef Samet, Ridha Abdelhédi

UR Electrochimie et Environnement, Ecole Nationale d'Ingénieurs de Sfax, BPW 3038 Sfax, Tunisia

ARTICLE INFO

ABSTRACT

Electrochemical oxidation of O-Toluidine (OT) was studied by galvanostatic electrolysis using lead dioxide (PbO$_2$) and boron-doped diamond (BDD) as anodes. The influence of operating parameters, such as current density, initial concentration of OT and temperature was investigated. Measurements of chemical oxygen demand were used to follow the oxidation. The experimental data indicated that on PbO$_2$ and BDD anodes, OT oxidation takes place by reaction with electrogenerated hydroxyl radicals and is favoured by low current density and high temperature. Furthermore, BDD anodes offer significant advantages over PbO$_2$ in terms of current efficiency and oxidation rate.

1. Introduction

Effluents from textile and paper industries contain large quantities of organic compounds and reactive dyes. These non-biodegradable pollutants must be treated before water discharge.

The commonly employed methods for colour removal are adsorption [1], coagulation [2], chemical oxidation with ozone [3] and advanced oxidation processes [4–6]. However, these processes are quite expensive and involve several operational problems. For these reasons, there has been an increasing interest in the use of new methods such as electrochemical oxidation [7,8].

Many studies have been carried out on electrochemical treatment of organic compounds and several anode materials have been tested. However, some of them have been shown to rapidly lose efficacy due to surface fouling, while others have only selectively oxidized pollutants without their complete incineration. Complete mineralization of organics to CO$_2$ has only been obtained using high oxygen overvoltage anodes, such as SnO$_2$ [9,10], PbO$_2$ [10–12] and BDD [13]. These electrodes produce hydroxyl radicals from the water discharge on their surfaces. For this kind of electrodes, very high current efficiencies may be obtained, and complete mineralization of the organic compounds can be achieved. However, common drawbacks of SnO$_2$ and PbO$_2$ are a short service-life [14], while BDD anodes have good chemical and electrochemical stability even in strong aggressive media, long life, and a wide potential window for water discharge. It has been demonstrated that many biorefractory compounds such as phenols [15,16], chlorophenols [11,17,18], pesticides [19,20], and industrial wastes [21] can be completely mineralized with high current efficiency, even close to 100%, using BDD anodes.

O-Toluidine was chosen as model substrate because it was largely used in the production of azo-dyes but was biorefractory and the chemical oxidation process, such as ozone [25] has some drawbacks including the production of large quantities of sludge or the high cost of ozone.

The aim of this work was to investigate and to compare the behaviour of BDD and PbO$_2$ anodes during bulk oxidation of OT. Furthermore, the influence of the main operating parameters, such as current density, concentration and temperature affecting OT oxidation, has been investigated for each electrode.

2. Experimental

2.1. Preparation of the Ta/PbO$_2$ electrode

The deposit of lead dioxide was made by electrochemical oxidation of an aqueous solution of lead nitrate on a rectangular tantalum plate. Tantalum has been chosen for reasons of chemical and electrochemical stability. From the potential–pH equilibrium data, tantalum undergoes passivation on contact with aqueous solution by formation of a non-conducting oxide layer Ta$_2$O$_5$ [26]. The tantalum surface is chemically stripped for 30 s in 40% hydrofluoric acid at room temperature. This chemical treatment dissolves the layer of tantalum oxide. The lead dioxide was galvanostatically deposited

using a single compartment cell ($V = 200\,cm^3$) thermoregulated at 65 °C. The anolyte was an aqueous solution containing lead nitrate at a concentration of 1 M. The cathode was a cylindrical mesh made of platinum. The deposition of PbO_2 was carried out for 2.5 h, using an anodic current density of $20\,mA\,cm^{-2}$. The average mass of PbO_2 was $0.18\,g\,cm^{-2}$. The deposit obtained is mat grey, adherent, regular and uniform.

2.2. Boron-doped diamond Si/BDD electrodes

The boron-doped diamond electrodes were kindly supplied by CSEM (Centre Swiss d'Electronique et de Microtechnique, Neuchâtel, Switzerland). It was synthesized by the hot filament chemical vapour deposition technique (HF-CVD) [27] on single-crystal p-type Si(1 0 0) wafers (1–3 mΩ cm, Siltronix). The doping level of boron in the diamond layer, expressed as B/C ratio, was about 3500 ppm. The resulting diamond film thickness was about 1 μm with a resistivity of 10–30 mΩ cm. The electrode area is $6\,cm^2$.

2.3. Electrolysis

The electrolyses of the OT aqueous solution have been carried out in a two compartments thermostatted cell under different current densities, temperatures and OT concentrations. BDD and PbO_2 were used as anode. The cathode was a graphite bar ($\varphi = 1\,cm$; $L = 6\,cm$) placed in a porous ceramic cylinder (Norton, RA 84) containing 1 M sulfuric acid solution. The anode was placed in front of the cathode. The geometric working surface of each anode was $6\,cm^2$.

Chemical oxygen demand (COD) was determined using the Reactor Digestion Method based on the method of acidic oxidation by bichromate.

The instantaneous current efficiency (ICE) of the electrolysis, which was an average value, was calculated from the values of the COD using the relationships [22].

$$ICE = \frac{COD_t - COD_{t+\Delta t}}{8 I \Delta t} FV \tag{1}$$

where COD_t and $COD_{t+\Delta t}$ are the chemical oxygen demands at times t and $t + \Delta t$ (in $g\,O_2\,L^{-1}$), respectively, and I is the current (A), F was the Faraday constant ($96487\,C\,mol^{-1}$), V is the volume of the electrolyte (L).

3. Results and discussion

3.1. Electrolysis on PbO_2 anode

3.1.1. Effect of current density

Fig. 1 shows the trend of the COD/COD_0 ratio and current efficiency during the anodic oxidation of 10^{-4} M of OT on the PbO_2 electrode at different current densities.

At high current density ($100\,mA\,cm^{-2}$) the efficiency and COD removal were lower due to an increase in the parasitic reaction of oxygen evolution (Eq. (1)), as already found [23] during OT degradation on a Ta/PbO_2 anode and probably to the reaction of peroxodisulfuric acid formation (Eq. (2)) [24].

$$2H_2O \rightarrow O_2 + 4H^+ + 4e^- \tag{2}$$

$$2H_2SO_4 \rightarrow H_2S_2O_8 + 2H^+ + 2e^- \tag{3}$$

3.1.2. Effect of the initial OT concentration

Fig. 2 shows the effect of the initial concentration of OT on the trend of COD/COD_0 ratio and ICE during galvanostatic electrolysis ($j = 20\,mA\,cm^{-2}$) at 50 °C.

It can be observed that the degradation increases with the decrease of OT concentration. Furthermore, COD decreased expo-
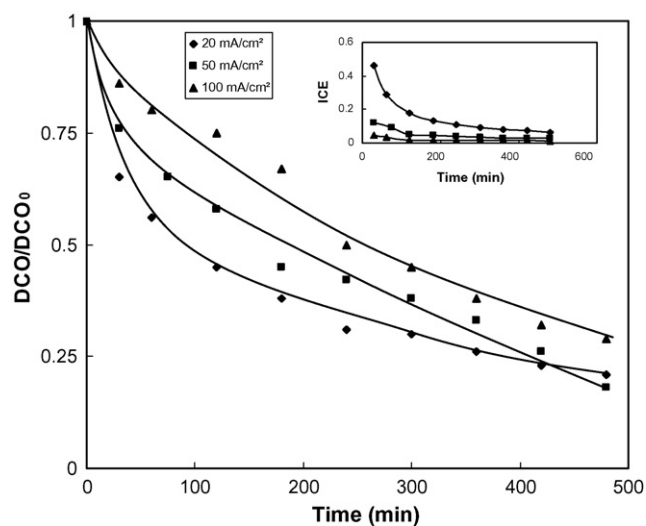

Fig. 1. Influence of applied current density: (♦) $j = 20\,mA\,cm^{-2}$; (■) $j = 50\,mA\,cm^{-2}$; (▲) $j = 100\,mA\,cm^{-2}$ on the trends of COD and ICE during electrolysis of 10^{-4} M OT; electrolyte 0.15 M Na_2SO_4, using PbO_2 anode. $T = 50$ °C and pH 6.

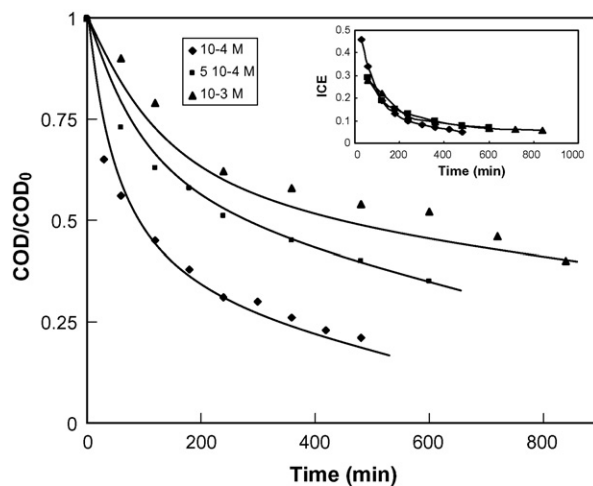**Fig. 2.** Influence of the initial OT concentration (♦) 10^{-4} M; (■) 5×10^{-4} M; (▲) 10^{-3} M on the trends of COD during electrolysis, using PbO_2 anode; electrolyte: 0.15 M Na_2SO_4; $j = 20\,mA\,cm^{-2}$; $T = 50$ °C and pH 6.

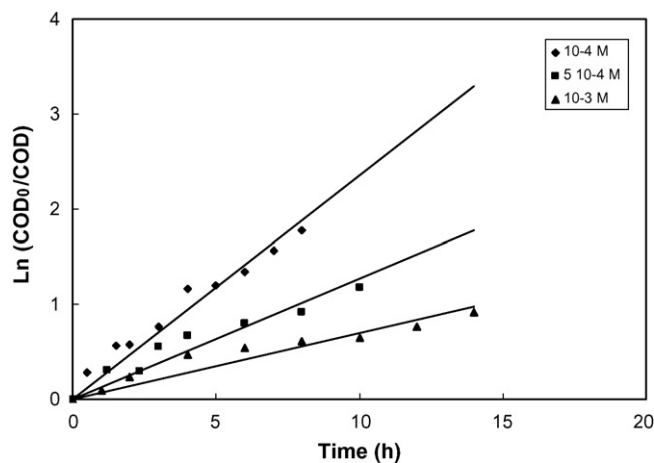**Fig. 3.** Linear regression for OT disappearance with time during electrochemical oxidation on a Ta/PbO_2 anode for different concentrations: (♦) 10^{-4} M; (■) 5×10^{-4} M; (▲) 10^{-3} M; $j = 20\,mA\,cm^{-2}$, $T = 50$ °C and pH 6.
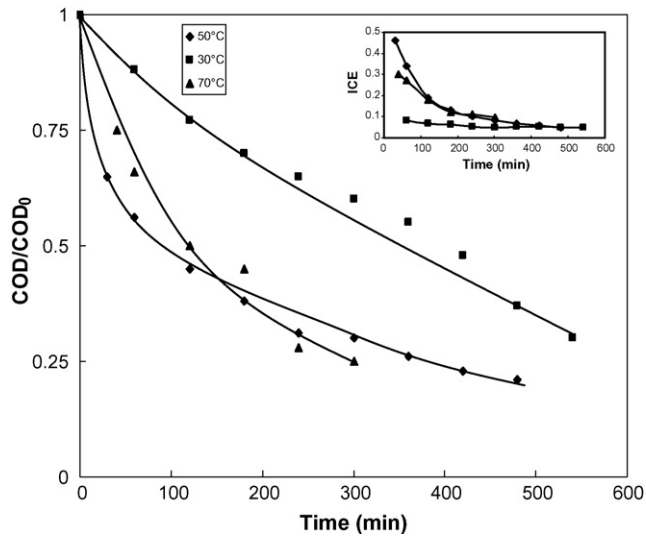
Fig. 4. Influence of temperature: (■) $T = 30\,^\circ C$; (♦) $T = 50\,^\circ C$, (▲) $T = 70\,^\circ C$ on the trends of COD during electrolysis of 10^{-4} M OT; electrolyte 0.15 M Na_2SO_4; using PbO_2 anode; $j = 20\,mA\,cm^{-2}$ and pH 6.
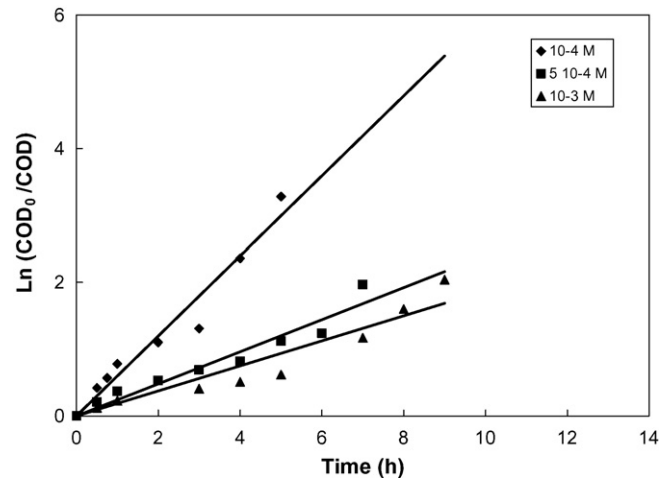

Fig. 7. Linear regression for OT disappearance with time during electrochemical oxidation on a BDD anode for different concentrations: (♦) 10^{-4} M; (■) 5×10^{-4} M; (▲) 10^{-3} M; $j = 50\,mA\,cm^{-2}$, $T = 50\,^\circ C$ and pH 6.
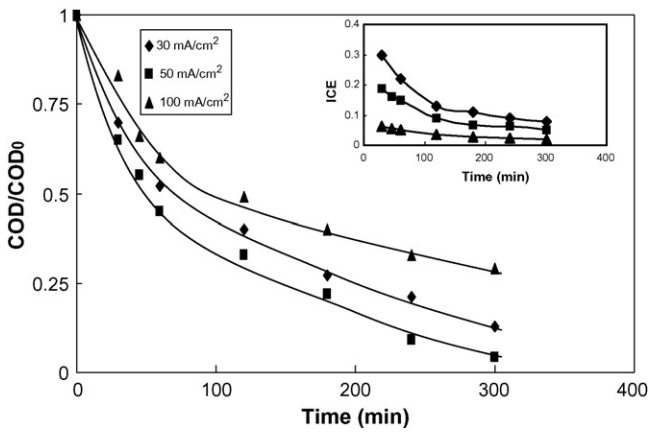

Fig. 5. Influence of applied current density: (♦) $j = 30\,mA\,cm^{-2}$; (■) $j = 50\,mA\,cm^{-2}$; (▲) $j = 100\,mA\,cm^{-2}$ on the trends of COD and ICE during electrolysis of 10^{-4} M OT; electrolyte 0.15 M Na_2SO_4; using BDD anode. $T = 50\,^\circ C$ and pH 6.

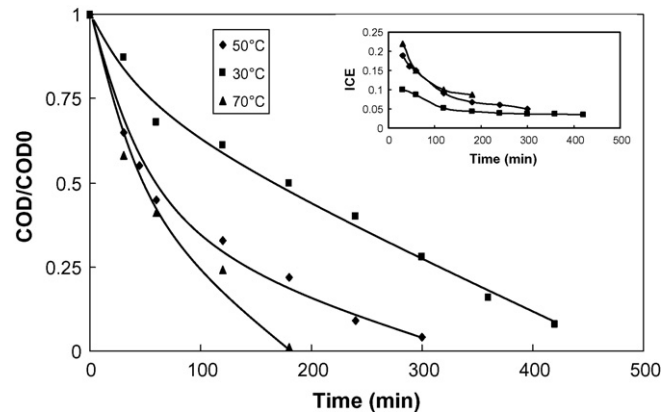**Fig. 8.** Influence of temperature (■) $T = 30\,^\circ C$; (♦) $T = 50\,^\circ C$, (▲) $T = 70\,^\circ C$ on the trends of COD and during electrolysis of 10^{-4} M OT; electrolyte 0.15 M Na_2SO_4, using BDD anode; $j = 50\,mA\,cm^{-2}$.
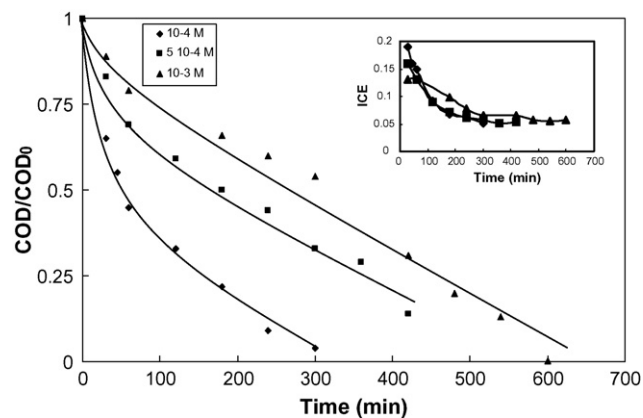
Fig. 6. Influence of the initial OT concentration: (♦) 10^{-4} M; (■) 5×10^{-4} M; (▲) 10^{-3} M on the trends of COD during electrolysis, using BDD anode; electrolyte: 0.15 M Na_2SO_4; $T = 50\,^\circ C$; $j = 50\,mA\,cm^{-2}$ and pH 6.

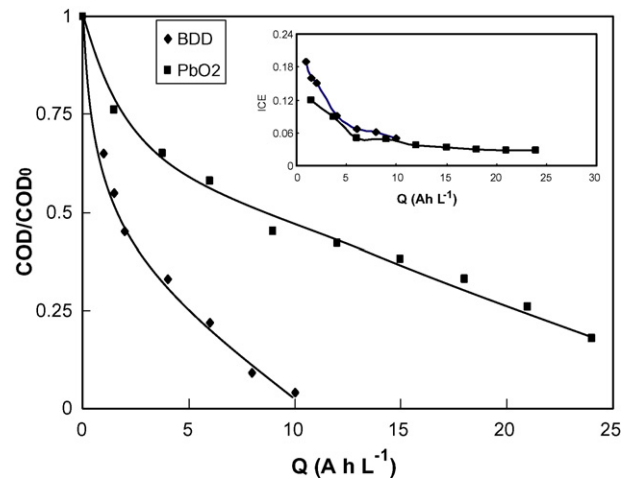**Fig. 9.** Comparison of the trend of COD during the oxidation of 10^{-4} M OT in 0.15 M Na_2SO_4, using (♦) BDD and (■) PbO_2 anode; $j = 50\,mA\,cm^{-2}$. $T = 50\,^\circ C$ and pH 6.

nentially and ICE was below 100%. This indicated that the oxidation is under mass transport control. In fact the theoretical model developed by Panizza et al. [24] showed that:

$$j_{app} < j_{lim} \ \text{under current control} \ \ \text{COD}(t) = \text{COD}^0 \left(1 - \frac{\alpha A k_m}{V} t\right)$$

$$(4)$$

$j_{app} > j_{lim}$ under mass transport control

$$\text{COD}(t) = \alpha \, \text{COD}^0 \exp\left(-\frac{A k_m}{V} t + \frac{1-\alpha}{\alpha}\right) \tag{5}$$

where j_{lim} and j_{app} are the limiting current density and the applied current density, respectively. $\alpha = j/j_{lim}$, V = cell volume (m^3), k_m = mass transport coefficient (m s^{-1}), A = electrode area (m^2) and COD^0 = initial COD (mol O$_2$ m^{-3}).

The variation of COD with time (see Fig. 2) showed a pseudo first-order kinetic, typical of reactions controlled by mass transport. Considering that the rate equation of this reaction can be written as:

$$\frac{d\text{COD}}{dt} = -k[\text{OH}^\bullet]^\alpha \text{COD} = -k_{app}\text{COD} \tag{6}$$

We suppose that hydroxyl radicals concentration is constant during the electrolysis ($k[\text{OH}^\bullet]^\alpha = k_{app}$). α is the reaction order relating to the hydroxyl radicals, k the real rate constant and k_{app} is the apparent rate constant. The above equation can be solved as follows:

$$\ln \frac{\text{COD}^0}{\text{COD}} = -k_{app} t = -k_m \frac{A}{V} t$$

Fig. 3 shows that $\ln \text{COD}^0/\text{COD}$ increases linearly with time, confirming a mass transport process.
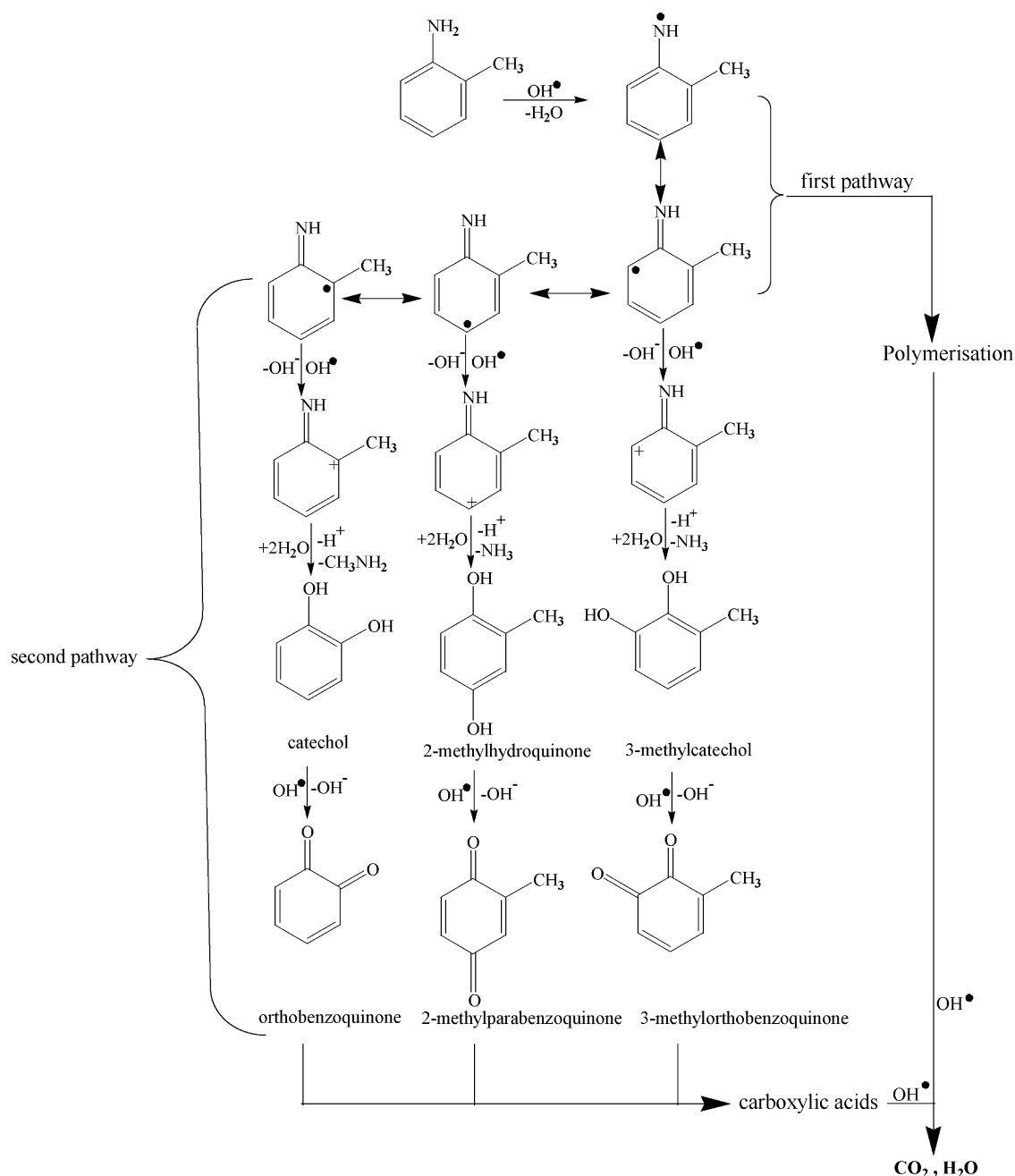

Fig. 10. Proposed reaction mechanism for the electrochemical oxidation of OT.

3.1.3. Effect of temperature

Fig. 4 shows the influence of temperature on the variation of COD/COD^0, during galvanostatic electrolysis ($j = 20\ \mathrm{mA\ cm^{-2}}$). The analysis of this figure shows that COD removal increased with temperature. However, at temperature 70 °C there was an anomaly during the first 5 h of electrolysis, this result can be probably explained by a polymerization of OT on PbO_2 anode which was favoured at high temperature.

3.2. Electrolysis on BDD anode

3.2.1. Effect of current density

Fig. 5 shows the trend of the COD and current efficiency during the oxidation of 10^{-4} M of OT at BDD electrode at different current densities. An increase of the current density resulted in a decrease of the oxidation rate because of the side reactions of oxygen evolution and peroxodisulfates formation, similar to the result found at the PbO_2 anode [24].

3.2.2. Effect of initial OT concentration

Fig. 6 shows the trend of the OT concentration during the oxidation of OT on BDD at $50\ \mathrm{mA\ cm^{-2}}$. This figure reveals an evolution similar to those obtained at the Ta/PbO_2 where the degradation rate was more significant as the concentration was small. In other terms the kinetics of degradation of OT was controlled by mass transport suggesting a pseudo first-order kinetic as in the case of Ta/PbO_2 anode (Fig. 7).

3.2.3. Effect of temperature

Fig. 8 shows the variation of COD according to the time of electrolysis of the OT at various temperatures. This figure shows that the higher was the temperature the better was the oxidation. With a temperature of 70 °C the complete OT mineralization was reached at the end of 180 min while at a temperature of 30 °C mineralization was reached only at the end of 420 min. This shows that the more the temperature was significant the more the oxidation of the organic pollutant was effective.

3.3. Comparison between two materials of electrode: PbO_2 and BDD

Fig. 9 shows the comparison of the trend of COD/COD_0 ratio during the oxidation of 10^{-4} M OT using PbO_2 and BDD anodes at a current density of $50\ \mathrm{mA\ cm^{-2}}$ and at 50 °C. It can be observed that after $10\ \mathrm{Ah\ L^{-1}}$, the percent removal of COD can reach 95% on BDD anode whereas it was only about 50% on PbO_2 anode. Furthermore, the ICE measured during the oxidation of OT with the BDD was always higher than that of the ICE obtained using the PbO_2 (inset of Fig. 9).

This result can be related to the adsorption properties of these two materials. In fact, it is well known that BDD anode has weak adsorption properties compared with PbO_2 anode, thus hydroxyl radicals electrogenerated on BDD anode were very weakly adsorbed and consequently more reactive towards organic oxidation reactions [22]. We can conclude that the BDD anode was the most effective electrode to degrade the OT.

Taking into account the effect of the hydroxyl radicals which are very powerful oxidizing agents able to react with organics leading to the dehydrogenated or hydroxylated derivatives till their complete mineralization (i.e., their conversion into CO_2, water and inorganic ions), a general reaction sequence for the electrochemical degradation of OT is proposed in the Fig. 10.

4. Conclusion

In this paper, the electrochemical oxidation of OT on different electrode materials such as the PbO_2 and BDD anodes has been studied. The results of bulk electrolysis performed under different experimental conditions have shown the following:

- Using the lead dioxide anode and the BDD, the mineralization of OT was obtained independently of the applied current density, due to the production of hydroxyl radicals on the electrode surface during electrolysis in the potential region of water oxidation.
- OT oxidation was a diffusion-controlled process and faster COD removal was obtained at low current densities.
- A comparison of the data obtained with the two electrode materials, each at its optimum experimental conditions, showed that faster OT mineralization and higher current efficiency were achieved using the BDD anode.
- During the OT oxidation, an increase in temperature significantly improves the percentage of OT elimination.
- The results of bulk electrolyses confirm the advantages of the BDD over the PbO_2.

References

[1] A. Bousher, X. Shen, R. Edyvean, Removal of coloured organic matter by adsorption onto low-cost waste materials, Water Res. 31 (1997) 2084–2092.

[2] D.H. Bache, M.D. Hossain, S.H. Al-Ani, P.J. Jackson, Optimum coagulation conditions for a coloured water in terms of floc size, density and strength, Water Supply 9 (1991) 93–102.

[3] M. Muthukumar, D. Sargunamani, N. Selvakumar, J.V. Rao, Optimisation of ozone treatment for colour and COD removal of acid dye effluent using central composite design experiment, Dyes Pigments 63 (2004) 127–134.

[4] S. Meric, D. Kaptan, T. Olmez, Color and COD removal from wastewater containing Reactive Black 5 using Fenton's oxidation process, Chemosphere 54 (2004) 435–441.

[5] A. Aleboyeh, Y. Moussa, H. Aleboyeh, Kinetics of oxidative decolourisation of Acid Orange 7 in water by ultraviolet radiation in the presence of hydrogen peroxide, Sep. Purif. Technol. 43 (2005) 143–148.

[6] U. Bali, E. Catalkaya, F. Sengul, Photodegradation of reactive black 5, direct red 28 and direct yellow12 using UV, UV/H_2O_2 and $UV/H_2O_2/Fe^{2+}$: a comparative study, J. Hazard. Mater. 114 (2004) 159–166.

[7] M. Ceron-Rivera, M.M. Davila-Jimenez, M.P. Elizalde-Gonzalez, Degradation of the textile dyes Basic yellow 28 and Reactive black 5 using diamond and metal alloys electrodes, Chemosphere 55 (2004) 1–10.

[8] A. Fernandes, A. Mora, M. Magrinho, A. Lopes, I. Goncalves, Electrochemical degradation of C. I. Acid Orange 7, Dyes & Pigments 61 (2004) 287–296.

[9] C. Comninellis, C. Pulgarin, Electrochemical oxidation of phenol for wastewater treatment using SnO_2 anodes, J. Appl. Electrochem. 23 (1993) 108–112.

[10] A.M. Polcaro, S. Palmas, F. Renoldi, M. Mascia, On the performance of SnO_2 and PbO_2 anodes on electrochemical degradation of chlorophenol for wastewater treatment, J. Appl. Electrochem. 29 (1999) 147–151.

[11] L. Gherardini, P.A. Michaud, M. Panizza, C. Comninellis, N. Vatistas, Electrochemical oxidation of 4-chlorophenol for wastewater treatment. Definition of normalized current efficiency, J. Electrochem. Soc. 148 (2001) D78–D82.

[12] Y. Samet, S. Chaabane Elaoud, S. Ammar, R. Abdelhedi, Electrochemical degradation of 4-chloroguaiacol for wastewater treatment using PbO_2 anodes, J. Hazard. Mater. B138 (2006) 614–619.

[13] M. Panizza, G. Cerisola, Application of diamond electrodes to electrochemical processes, Electrochim. Acta 51 (2005) 191–199.

[14] B. Correa-Lozano, C. Comninellis, A. DeBattisti, Service life of $Ti/SnO_2–Sb_2O_5$ anodes, J. Appl. Electrochem. 27 (1997) 970–974.

[15] P. Canizares, M. Diaz, J.A. Dominguez, J. Garcia-Gomez, M.A. Rodrigo, Electrochemical oxidation of aqueous phenol wastes on synthetic diamond thin-film electrodes, Ind. Chem. Res. 41 (2002) 4187–4194.

[16] J. Iniesta, P.A. Michaud, M. Panizza, G. Cerwasola, A. Aldaz, C. Comninellis, Electrochemical oxidation of phenol at boron-doped diamond electrode, Electrochim. Acta 46 (2001) 3573–3578.

[17] B. Boye, P.A. Michaud, B. Marselli, M.M. Dieng, E. Brillas, C. Comninellis, Anodic oxidation of 4-chlorophenoxyacetic acid on synthetic boron-doped diamond electrodes, New Diamond Front. Carbon Technol. (2002) 63–72.

[18] P. Canizares, J. Garcia-Gomez, C. Saez, M.A. Rodrigo, Electrochemical oxidation of several chlorophenols on diamond electrodes. Part I. Reaction mechanism, J. Appl. Electrochem. 33 (2003) 917–927.

[19] E. Brillas, B. Boye, I. Sires, J.A. Garrido, R.M. Rodriguez, C. Arias, P.L. Cabot, C. Comninellis, Electrochemical destruction of chlorophenoxy herbicides by anodic oxidation and electro-Fenton using a boron-doped diamond electrode, Electrochim. Acta 49 (2004) 4487–4496.

[20] A.M. Polcaro, M. Mascia, S. Palmas, A. Vacca, Electrochemical degradation of diuron and dichloroaniline at BDD electrode, Electrochim. Acta 49 (2004) 649–656.

[21] M. Panizza, P.A. Michaud, G. Cerwasola, C. Comninellis, Electrochemical treatment of wastewater containing organic pollutants on boron-doped diamond electrodes. Prediction of specific energy consumption and required electrode area, Electrochem. Commun. 3 (2001) 336.

[22] M. Panizza, G. Cerisola, Influence of anode material on the electrochemical oxidation of 2-naphtol. Part 2. Bulk electrolysis experiments, Electrochim. Acta 49 (2004) 3221–3226.

[23] N.B. Tahar, A. Savall, Mechanistic aspects of phenol electrochemical degradation by oxidation on a Ta/PbO$_2$ anode, J. Electrochem. Soc. 145 (1998) 3427.

[24] M. Panizza, P.A. Michaud, G. Cerisola, Ch. Comninellis, Anodic oxidation of 2-naphtol at boron-doped diamond electrodes, J. Electroanal. Chem. 507 (2001) 206–214.

[25] S. Gul, O. Serindag, H. Boztepe, Effects of ozonation on COD elimination of aromatic compounds in aqueous solution, Turk. J. Chem. 23 (1999) 21–26.

[26] M. Pourbaix, Atlas d'équilibres électrochimiques à 25 °C, Gautier-Villars, Paris, 1963.

[27] A. Perret, W. Haenni, N. Skinner, X.M. Tang, D. Gandini, Ch. Comninellis, B. Correa, G. Foti, Electrochemical behavior of synthetic diamond thin film electrodes, Diamond Relat. Mater. 8 (1999) 820–823.